

Measuring the Cosmological Geometry from the Lyman Alpha Forest along Parallel Lines of Sight

Patrick McDonald and Jordi Miralda-Escudé¹

Univ. of Pennsylvania, Dept. of Physics and Astronomy

¹ Alfred P. Sloan Fellow

ABSTRACT

We discuss the feasibility of measuring the cosmological geometry using the redshift space correlation function of the Ly α forest in multiple lines of sight, as a function of angular and velocity separation. The geometric parameter that is measured is $f(z) \equiv c^{-1}H(z)D(z)$, where $H(z)$ is the Hubble constant and $D(z)$ the angular diameter distance at redshift z . The correlation function is computed in linear theory. We describe a method to measure it from observations with the Gaussianization procedure of Croft et al. (1998) to map the observed Ly α forest transmitted flux to an approximation of the linear density field. The effect of peculiar velocities on the *shape* of the recovered power spectrum is pointed out. We estimate the error in recovering the $f(z)$ factor from observations due to the variance in the Ly α absorbers. We show that ~ 20 pairs of quasars (separations $< 3'$) are needed to distinguish a flat $\Omega_0 = 1$ universe from a universe with $\Omega_0 = 0.2$, $\Omega_\Lambda = 0.8$. A second parameter that is obtained from the correlation function of the Ly α forest is $\beta \simeq \Omega(z)^{0.6}/b$ (affecting the magnitude of the peculiar velocities), where b is a linear theory bias of the Ly α forest. The statistical error of $f(z)$ can be reduced if b can be determined independently from numerical simulations, reducing the number of quasar pairs needed for constraining cosmology to approximately six. On small scales, where the correlation function is higher, $f(z)$ should be measurable with fewer quasars, but non-linear effects must then be taken into account. The anisotropy of the non-linear redshift space correlation function as a function of scale should also provide a precise quantitative test of the gravitational instability theory of the Ly α forest.

Subject headings: cosmology: theory — intergalactic medium — large-scale structure of universe — quasars: absorption lines

1. Introduction

One of the methods to measure the parameters of the global cosmological metric of the universe is to observe the angular size and the redshift extent of a set of objects, which can be assumed to be spherically symmetric and to follow the Hubble expansion on average (Alcock

& Paczyński 1979). More generally, this geometric factor can be measured from a correlation function of any set of objects depending on angular separation and redshift difference, by requiring that the correlation is isotropic. It has long been known that this measurement at high redshift is sensitive primarily to the cosmological constant (Alcock & Paczyński 1979). However, generally the correlation of objects is due to gravitational collapse, and the peculiar velocities make the correlation function in redshift space anisotropic (Kaiser 1987). The effect of peculiar velocities must be taken into account before the method can be applied.

Recently, a method has been developed to recover the power spectrum of mass fluctuations from quasar absorption spectra, by measuring the one-dimensional power spectrum and converting it to the desired three-dimensional power spectrum (Croft et al. 1998, hereafter CWKH). This method suffers from peculiar velocity distortions similar to those which distort the isotropy of the correlation in redshift space. Here, we consider the accuracy in the measurement of the redshift space correlation function from the Ly α forest in nearby pairs of quasars. We show that it is possible to disentangle the effects of geometry and peculiar velocities, and recover the power spectrum of mass fluctuations from the correlations in the Ly α forest. We also demonstrate that the peculiar velocities are important for correctly deriving the shape of the power spectrum.

In §2 we summarize equations describing the cosmological geometry, discuss the linear theory correlation function in redshift space, and comment on the effect of peculiar velocities on the shape of the power spectrum. In §3 we use a random line model to estimate the error in the measurement of $f(z)$ from a given number of observed quasar spectra. The discussion is given in §4. Figures 6-9 contain the main results of this paper.

2. Linear Theory of the Lyman Alpha Forest Correlation Function

2.1. Cosmological Geometry

The following is a short summary of the cosmological equations we shall use (these have been discussed earlier in several papers, e.g., Matsubara & Suto 1996, Ballinger et al. 1997). Observations directly measure the redshift and angular position of each object. We write the angular and redshift separation between two objects as $(\Delta z, \Delta\theta)$. The redshift is caused both by Hubble flow velocities (v_h) and peculiar velocities along the line of sight (v_p). The total velocity separation along the line of sight is $\Delta v_{\parallel} = c\Delta z/(1+z) = \Delta v_h + \Delta v_p$. It is also convenient to define a perpendicular velocity separation, $\Delta v_{\perp} = cf(z)\Delta\theta$, where $f(z)$ is a dimensionless function of redshift that includes all the dependence on the global cosmological metric. With the assumption of isotropy, the real space two-point correlation function of density fluctuations $\xi_r(\Delta v_h, \Delta v_{\perp})$ must be a function of $\sqrt{\Delta v_h^2 + \Delta v_{\perp}^2}$ only. If ξ_r could be measured, it would be a relatively straightforward matter to measure $f(z)$ by simply demanding isotropy. In reality, distances cannot be measured accurately and only the redshift space correlation function ξ can be determined, which is affected by peculiar velocities. The peculiar velocities introduce an anisotropy in ξ of the

same order as the difference in $f(z)$ between various cosmological models.

The quantity $f(z)$ is predicted for any cosmological model. If the present density of matter (in units of the critical density) is Ω_0 , and considering also a negative pressure component with density Ω_Λ and equation of state $p = w\rho$ (the case $w = -1$ is the cosmological constant), we have, for an open universe,

$$f(z) = \frac{E(z) \sinh [\sqrt{\Omega_R} \int_0^z (dz/E(z))]}{(1+z)\sqrt{\Omega_R}}, \quad (1)$$

and for a flat universe,

$$f(z) = \frac{E(z) \int_0^z (dz/E(z))}{(1+z)}. \quad (2)$$

Here, $\Omega_R = 1 - \Omega_0 - \Omega_\Lambda$ ($\Omega_R = 0$ for a flat universe), and

$$E(z) = \sqrt{\Omega_0(1+z)^3 + \Omega_R(1+z)^2 + \Omega_\Lambda(1+z)^{3(1+w)}}. \quad (3)$$

Figure 1 shows predictions for $f(z)$.

2.2. The Correlation Function in Redshift Space

In linear theory, the redshift space correlation function of the density field is given by (Kaiser 1987; Lilje & Efstathiou 1989; Hamilton 1992; Fisher 1995)

$$\xi(\Delta v_\parallel, \Delta v_\perp) = \left(1 + \frac{2}{3}\beta + \frac{1}{5}\beta^2\right) \xi_0(s) - \left(\frac{4}{3}\beta + \frac{4}{7}\beta^2\right) \xi_2(s)P_2(\mu) + \left(\frac{8}{35}\beta^2\right) \xi_4(s)P_4(\mu), \quad (4)$$

where $s = \sqrt{\Delta v_\parallel^2 + \Delta v_\perp^2}$, $\mu = \Delta v_\parallel/s$, $P_l(\mu)$ are the usual Legendre polynomials, and

$$\xi_l(s) = \frac{b^2}{2\pi^2} \int_0^\infty dk k^2 P(k) j_l [ks(1+z)/H(z)]. \quad (5)$$

The functions $j_l(x)$ are the usual spherical Bessel functions, and $P(k)$ is the power spectrum of the mass fluctuations. The parameter β is related to the linear theory bias b by $\beta = b^{-1} H(z)^{-1} (dD/dt)/D$, where D is the linear growth factor, $H(z)$ is the Hubble constant and t is the age of the universe [see Peebles 1993; $H(z)^{-1} (dD/dt)/D \simeq \Omega(z)^{0.6}$ is a good approximation in most models].

Equation (4) is valid only in linear theory, and the correlation function ξ could only be determined directly from observations if the linear density field, δ , were known. Only the fraction of the flux that is transmitted, F , can be determined along a line of sight from the Ly α forest spectrum in a quasar (we assume here that the quasar continuum has been fitted to a model, allowing the transmitted flux fraction F to be measured at every pixel). We need a way to recover the linear density field δ from the observed F . In general, this cannot be done exactly since F is only known along a line of sight, and besides the chaotic nature of non-linear evolution limits the

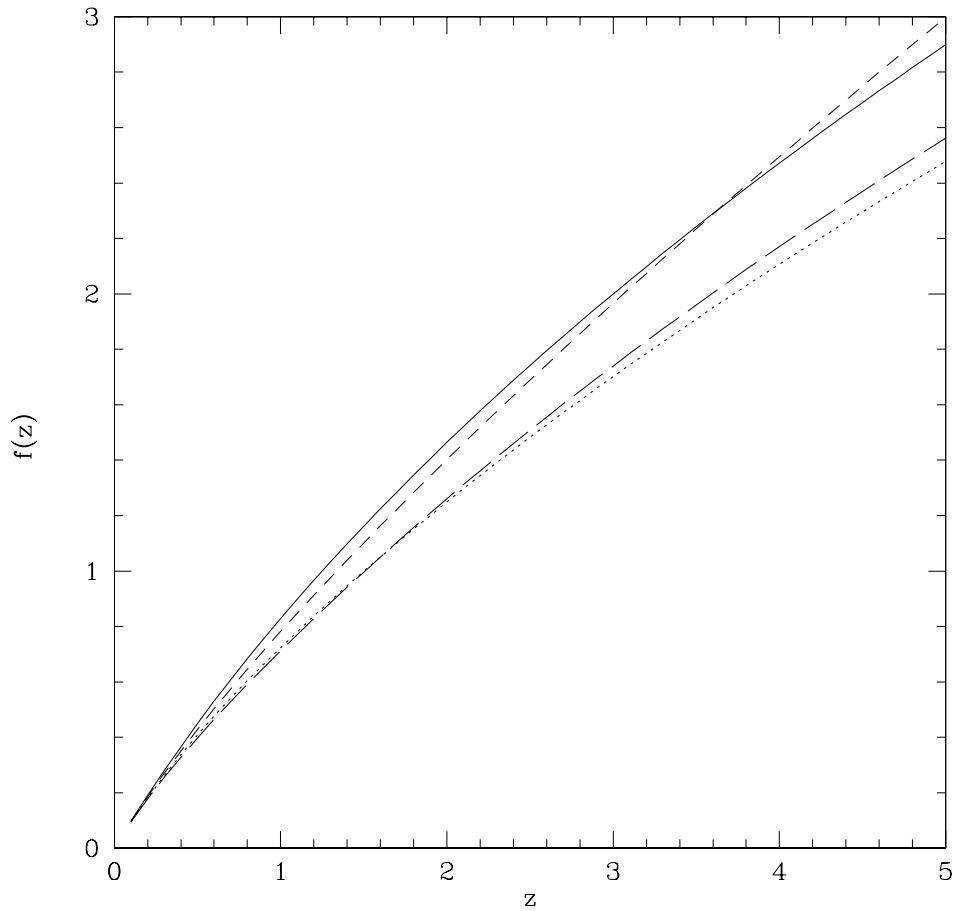


Fig. 1.— $f(z) \equiv \Delta v_{\perp}/(c\Delta\theta)$ computed for $\Omega_0 = 1.0$, $\Omega_{\Lambda} = 0.0$ (solid line), $\Omega_0 = 0.4$, $\Omega_{\Lambda} = 0.6$, $w = -1$ (long dashed line), $\Omega_0 = 0.3$, $\Omega_{\Lambda} = 0.0$ (short dashed line), and $\Omega_0 = 0.4$, $\Omega_{\Lambda} = 0.6$, $w = -2/3$ (dotted line).

accuracy to which δ can be recovered. Here, we adopt the Gaussianization procedure of CWKH (see also Weinberg 1992). Gaussianization assumes that the initial mass density fluctuations were Gaussian random and that evolution approximately preserves the rank order of densities, even as it distorts the distribution from a Gaussian. In the case of the Ly α forest, values of the observed flux decrement are mapped monotonically onto a new variable δ required to have the probability distribution function

$$P(\delta) = \frac{1}{\sqrt{2\pi\xi(0)}} \exp \left[-\frac{1}{2} \frac{\delta^2}{\xi(0)} \right]. \quad (6)$$

Of course, the fluctuation amplitude $\sqrt{\xi(0)}$ is not recovered by the assumption that the rank order is preserved. Computing the correlation function of the Gaussianized spectrum yields only the ratio $\tilde{\xi}(\Delta v, \Delta\theta) \equiv \xi(\Delta v, \Delta\theta)/\xi(0)$.

Once the new variable δ is obtained, the correlation function may be computed from observations through the usual estimator given by its definition: $\xi(\Delta\mathbf{v}) = \langle \delta(\mathbf{v}) \delta(\mathbf{v} + \Delta\mathbf{v}) \rangle$, where $\Delta\mathbf{v}$ symbolizes the vector separation $(\Delta v_{\parallel}, \Delta v_{\perp})$. The average is taken over all pairs of pixels separated by $\Delta\mathbf{v}$ in the spectra available. However, this is not necessarily the best estimator of ξ , and in general it should be better to examine the full 2-point joint probability distribution function. One of the main reasons for this is that the assumption that the density rank order is preserved should obviously break down at high optical depths, because the gas at high densities will typically be shocked and follow a highly stochastic evolution, developing small-scale structure. The spectrum will also be greatly affected by velocity caustics and thermal broadening, and when $\tau \gg 1$ the value of δ derived from Gaussianization will have large errors because of saturation. On the other hand, at low densities the evolution is much more regular, velocity caustics do not appear, and thermal broadening can be neglected, so there should be a good correspondence between the optical depth at a given velocity and the gas density at the corresponding point in space.

The 2-point distribution function for a Gaussian field is

$$P_2(\delta_1, \delta_2, \Delta\mathbf{v}) = \frac{1}{2\pi\sqrt{\xi(0)^2 - \xi(\Delta\mathbf{v})^2}} \exp \left[-\frac{1}{2} \frac{\xi(0)(\delta_1^2 + \delta_2^2) - 2\delta_1\delta_2\xi(\Delta\mathbf{v})}{\xi(0)^2 - \xi(\Delta\mathbf{v})^2} \right]. \quad (7)$$

This can be rewritten as

$$P_2(\delta_1, \delta_2, \Delta\mathbf{v}) = P(\delta_1) \frac{1}{\sqrt{2\pi\xi(0)(1 - \tilde{\xi}(\Delta\mathbf{v})^2)}} \exp \left\{ -\frac{1}{2} \frac{[\delta_2 - \tilde{\xi}(\Delta\mathbf{v})\delta_1]^2}{\xi(0)[1 - \tilde{\xi}(\Delta\mathbf{v})^2]} \right\}. \quad (8)$$

Thus, for every value of δ_1 , we can estimate $\tilde{\xi}(\Delta\mathbf{v})$ from the distribution of δ_2 conditional to the value of δ_1 . For example, one could estimate $\tilde{\xi}(\Delta\mathbf{v})$ from the median of δ_2 (or any other adequate percentile), and see how the result depends on δ_1 . If the method works, $\tilde{\xi}$ should be approximately independent of δ_1 for low values of δ_1 . Using instead $\xi(\Delta\mathbf{v}) = \langle \delta(\mathbf{v}) \delta(\mathbf{v} + \Delta\mathbf{v}) \rangle$ is equivalent to averaging the estimate of ξ over all values of δ_1 with equal weights.

2.3. The Effect of Peculiar Velocities on the Power Spectrum

In their reconstruction of the linear power spectrum from Ly α forest lines, CWKH neglect the effect of peculiar velocities on the shape of $P(k)$. This effect arises in the conversion from the measured one-dimensional power spectrum P_{1D} to the desired three-dimensional power spectrum P_{3D} . While the shape of P_{3D} is not affected by peculiar velocities in linear theory (Kaiser 1987), P_{1D} is affected as shown by Kaiser & Peacock (1991):

$$P_{1D}(k_{\parallel}) = \frac{1}{2\pi} \int_{k_{\parallel}}^{\infty} dk k P_{3D}(k) (1 + \beta k_{\parallel}^2/k^2)^2, \quad (9)$$

To demonstrate how this will affect the reconstruction of CWKH, we substitute a specific $P_{3D}(k)$ into equation (9), with various values of β . We use the cold dark matter power spectrum parameterization of Bardeen et al. (1986), with the coefficients of Ma (1996) (see §3.1 below), and the parameters: $\Omega = 1$, $h = 0.5$, $n = 1.0$. We then assume that the resulting P_{1D} is the one-dimensional power spectrum for the Ly α forest and attempt to reconstruct the three-dimensional power spectrum ignoring peculiar velocities (i.e., setting $\beta = 0$). This yields a new function $\tilde{P}_{3D}(k)$, different from the correct $P_{3D}(k)$ because of the effect of peculiar velocities, which is given by

$$\tilde{P}_{3D}(k) = P_{3D}(k)(1 + \beta)^2 - \int_k^{\infty} dk' \left[\frac{4\beta}{k'} P_{3D}(k') (1 + \beta \frac{k^2}{k'^2}) \right]. \quad (10)$$

The second term causes the change in the shape of $\tilde{P}_{3D}(k)$ relative to $P_{3D}(k)$. Figure 2 shows the results of this procedure for various values of β . The error in the reconstructed power spectrum grows with scale and eventually causes the results to become negative. The power spectrum used in this figure was smoothed by a Gaussian with radius $r_s = 0.24h^{-1} \text{ Mpc}^1$. CWKH found that this was necessary to match the $P(k)$ they reconstructed from simulations.

Thus, the shape of the mass power spectrum $P_{3D}(k)$ cannot be recovered until the parameter β is known. How can this parameter be determined? One could in principle attempt to determine β from observations in multiple lines of sight, as described in the next section. The anisotropy of the correlation function depends on the two parameters β and $f(z)$. But as we shall see, a very large amount of data will be required to measure both of them independently. If β can be predicted from theory, it should be much less difficult to determine the power spectrum and $f(z)$.

Linear theory would predict $b = 2$ for a constant temperature in the intergalactic medium, because the optical depth (which is the quantity that is modified by peculiar velocities in the mapping from real to redshift space) is proportional to the neutral hydrogen density, or the square of the gas density. In a photoionized medium, the gas temperature is determined by a

¹ The value of r_s quoted in CWKH (in the caption of their Fig. 2) was wrong by a factor 2π ; Croft 1998, priv. communication.

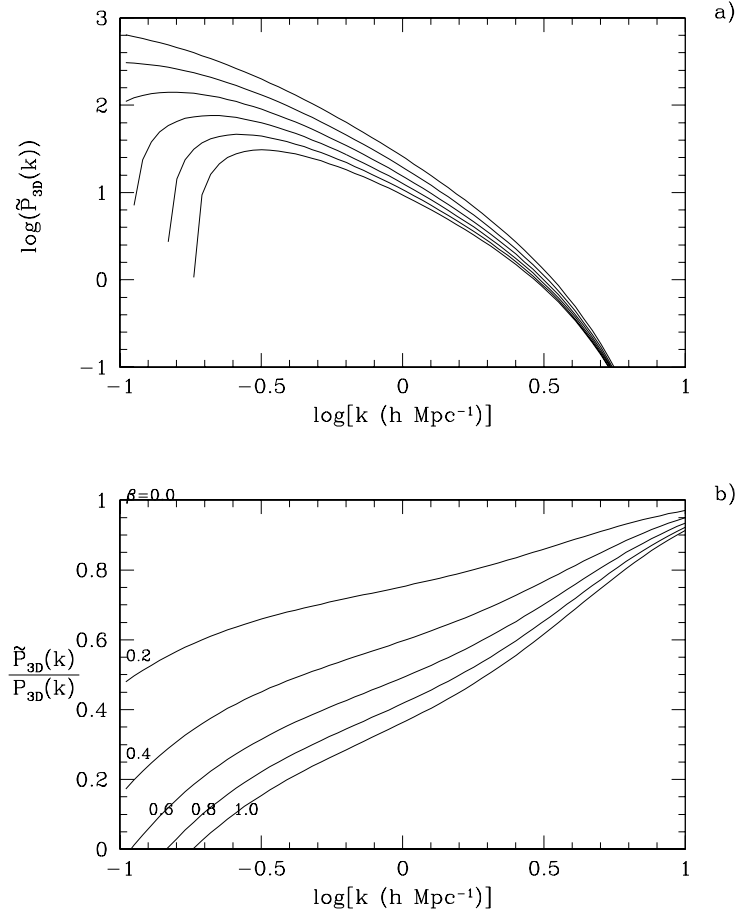


Fig. 2.— (a) The power spectrum as it would appear if reconstructed from $P_{1D}(k)$ while ignoring peculiar velocity effects. From top to bottom, $\beta = 0.0, 0.2, 0.4, 0.6, 0.8, 1.0$. The $\beta = 0$ line is the correct power spectrum. The normalization for all curves is fixed at large k , and a Gaussian cutoff has been applied. (b) The ratio of the reconstructed to the true power spectra.

balance of photoionization heating and adiabatic cooling. The heating rate is proportional to the recombination rate, $\alpha\rho$, and the adiabatic cooling is proportional to the temperature T . Since $\alpha \propto T^{-0.7}$, the relation $T \propto \rho^{0.6}$ is set up if the gas temperature is not affected by shocks or by reionization (see Hui & Gnedin 1997, Croft et al. 1997). This leads to a neutral hydrogen density proportional to $\alpha\rho^2 \propto \rho^{1.6}$, and therefore a Ly α forest bias $b = 1.6$. Since $\Omega(z) \simeq 1$ at $z \sim 3$ for viable models, $\beta \simeq 0.6$. However, in reality the bias depends on the relation of optical depth to the initial density on small scales, where non-linearities are important, and therefore the correct bias to use in equations (6), (9), and (10), where linear theory is applied to large scales using the Gaussianization approximation, could be substantially different. Numerical simulations can be used to calculate a better value for the Ly α forest bias (which will in general depend on redshift), but of course this will only be accurate if the simulations are modeling the structure of the Ly α forest correctly.

The effects of peculiar velocities on the recovery of the mass power spectrum have independently been pointed out in a recent paper by Hui (1998), which appeared as this paper was being completed.

3. Errors in the Measurement of the Ly α Forest Correlation

In this section, an estimate is obtained of the statistical error in measuring the parameters of the correlation function, due to the random nature of the absorption lines that appear in the spectra. A simple model of absorption lines will be used to generate random spectra that reproduce the characteristics of the individual Ly α forest absorption lines without the large scale correlation.

3.1. Parameterization of the Correlation Function

As discussed in §2, two parameters describe the anisotropy of the correlation function: $f(z)$, reflecting the effect of the cosmological geometry, and $\beta(z)$, incorporating the peculiar velocity effects. We also parameterize the shape of the power spectrum to a fitting formula for cold dark matter models,

$$P(k_s) = \frac{k_s^n [\ln(1 + \alpha_1 q) / \alpha_1 q]^2}{[1 + \alpha_2 q + (\alpha_3 q)^2 + (\alpha_4 q)^3 + (\alpha_5 q)^4]^{\frac{1}{2}}}, \quad (11)$$

where $q \equiv k_s / \Gamma(z)$. We have reexpressed the power spectrum in terms of $k_s = k(1+z)/H(z)$. The free parameters of this model for the shape of the power spectrum are n and $\Gamma(z)$ (given by $\Gamma(z) = (1+z)\Omega_0 h^2 / H(z)$). The formula is given by Bardeen et al. (1986), but we modify the parameters to the fit for $\Omega_b = 0.05$: $\alpha_1 = 2.205$, $\alpha_2 = 4.05$, $\alpha_3 = 18.3$, $\alpha_4 = 8.725$, and $\alpha_5 = 8.0$ (Ma 1996). In addition we include a smoothing parameter by multiplying the above formula by the factor $\exp(-k_s^2 v_s^2 / 2)$, with $v_s = r_s H(z) / (1+z) = 48 \text{ km s}^{-1}$ at $z = 3$. This is motivated by the

result of CWKH, who find that the Ly α forest has a power spectrum (after Gaussianization) that can be well approximated by a smoothed version of the power spectrum of the mass. We fix v_s (rather than r_s) to the same value for all models, since the observations always yield separations in terms of velocity.

In Figure 3, we display the computed $\tilde{\xi}(\Delta v, \Delta\theta)$ along the line of sight ($\Delta\theta = 0$), and at separations $\Delta\theta = 127''$ and $\Delta\theta = 300''$, at mean redshift $\langle z \rangle = 2.25$. Because of the Gaussianization, we measure $\tilde{\xi}(\Delta v, \Delta\theta) \equiv \xi(\Delta v, \Delta\theta)/\xi(0)$. The model parameters are $\Omega_0 = 1.0$, $\Omega_\Lambda = 0.0$, $h = 0.65$, $n = 1.0$, and $\beta = 0.6$. These parameters correspond to $f(z) = 1.61$, and $\Gamma(z) = 0.0036 \text{ (km/s)}^{-1}$. Also shown in the figure are the predictions for a model with $f(z) = 1.39$ (the value for $\Omega_0 = 0.4$, $\Omega_\Lambda = 0.6$), but with Γ , n , β and v_s unchanged.

3.2. Analysis of Random Spectra

In this subsection we use a random line model to estimate the noise in the measurement of $\tilde{\xi}(\Delta v, \Delta\theta)$. We create Ly α forest spectra using a code which produces lines by randomly distributing Voigt profiles with a specified distribution of column densities N and widths b . Figure 4 shows a piece of one of these spectra. We take a set of parameters that closely match the distribution in the observations (e.g., Kim et al. 1997). We will consider the mean redshift $\langle z \rangle = 2.25$. We set the number of lines per unit redshift with column density greater than 10^{14} cm^{-2} to be $N_{>14} = 50$, and set $f(N) \propto N^{-1.35}$ with a break to $N^{-1.7}$ at $\log(N) = 14.3$. We set the mean b-parameter of the Voigt profiles to be $\langle b \rangle = 30 \text{ km s}^{-1}$ with a Gaussian dispersion of $\sigma_b = 12 \text{ km s}^{-1}$ and a lower cutoff of $b_{cut} = 24 \text{ km s}^{-1}$.

A spectrum is generated by calculating the transmitted flux at discrete pixels from the list of randomly generated lines. We then make a transformation of the transmitted flux to a new variable δ , requiring that the probability distribution of δ is Gaussian (this is the Gaussianization procedure). Because the absorption lines are random, there should be no correlation at separations beyond the width of the individual components, so any correlation we measure at larger separations is due to noise. Figure 5 shows the resulting $\tilde{\xi}(\Delta v, 0)$ for a pair of lines. The self-correlation of the individual components due to their own width extends out to $\Delta v \simeq 170 \text{ km s}^{-1}$. The *rms* fluctuation around the mean $\tilde{\xi}$ is $\sigma_{\tilde{\xi}} \simeq 0.03$. The errors in ξ are obviously also correlated over $\sim 100 \text{ km s}^{-1}$ due to the width of the lines.

3.3. Estimation of Errors

We now estimate the errors in measuring parameters in the correlation function from a given set of quasar spectra. We consider first as an example the triplet of quasars of Crotts & Fang (1998), which have a useful redshift range $z \simeq 2.0 - 2.5$ and separations $\Delta\theta = 127''$, $147''$, and $177''$. The error bars we have computed for $\tilde{\xi}$ are not necessarily Gaussian, and certainly not

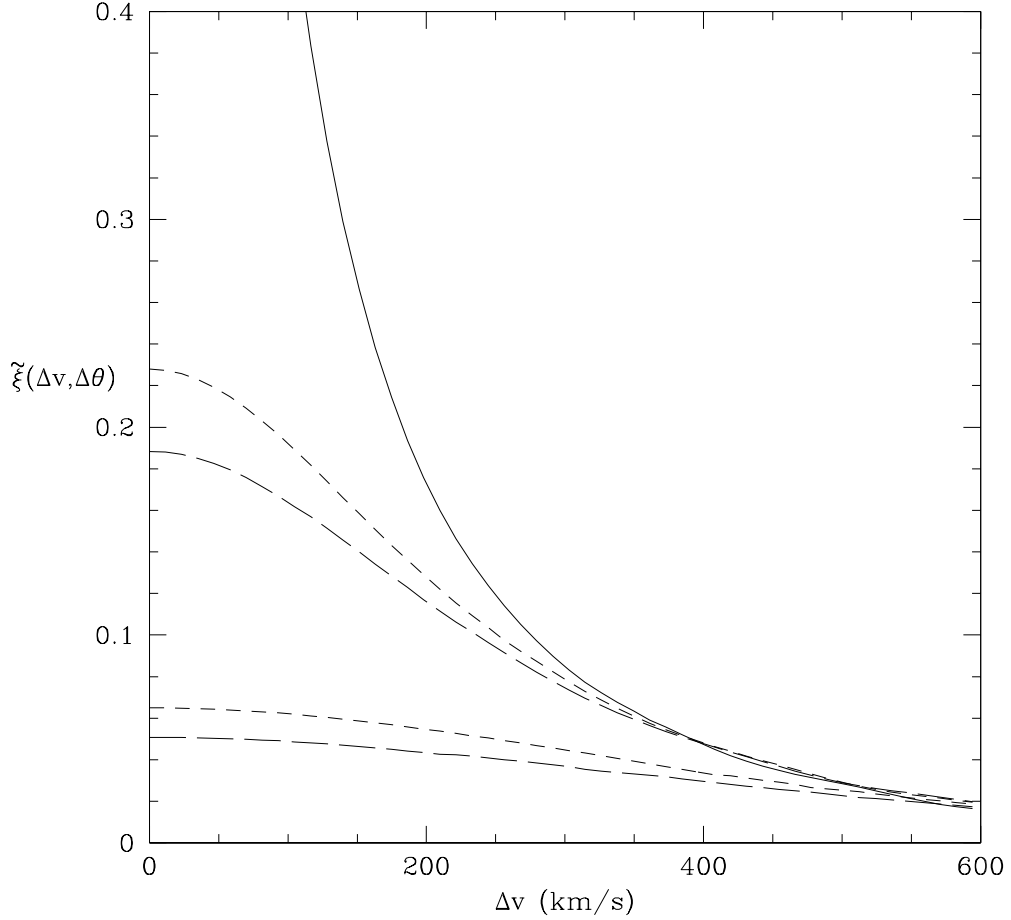


Fig. 3.— The solid and long dashed lines are predictions for a flat model with $\Omega_0 = 1.0$, $h = 0.65$, and $\beta = 0.6$ (giving $f(z) = 1.61$). The solid line is the correlation along the line of sight (normalized to $\tilde{\xi}(0,0) = 1$ because of Gaussianization). The upper dashed lines are for $\Delta\theta = 127''$, and the lower dashed lines are for $\Delta\theta = 300''$. The short dashed lines were produced by changing $f(z)$ to 1.39, appropriate for a flat $\Omega_\Lambda = 0.6$ model, *without* changing the power spectrum parameters or β (the line of sight correlation is the same in each case).

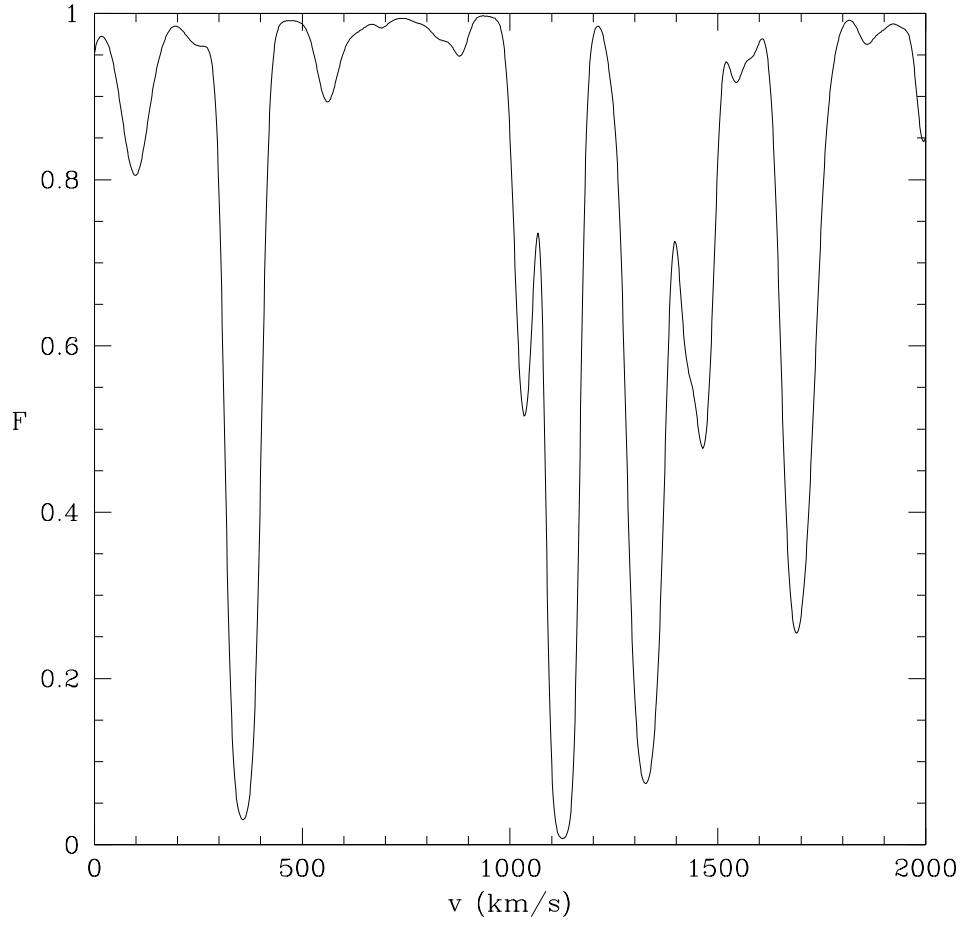


Fig. 4.— Flux vs. velocity for a randomly generated spectrum.

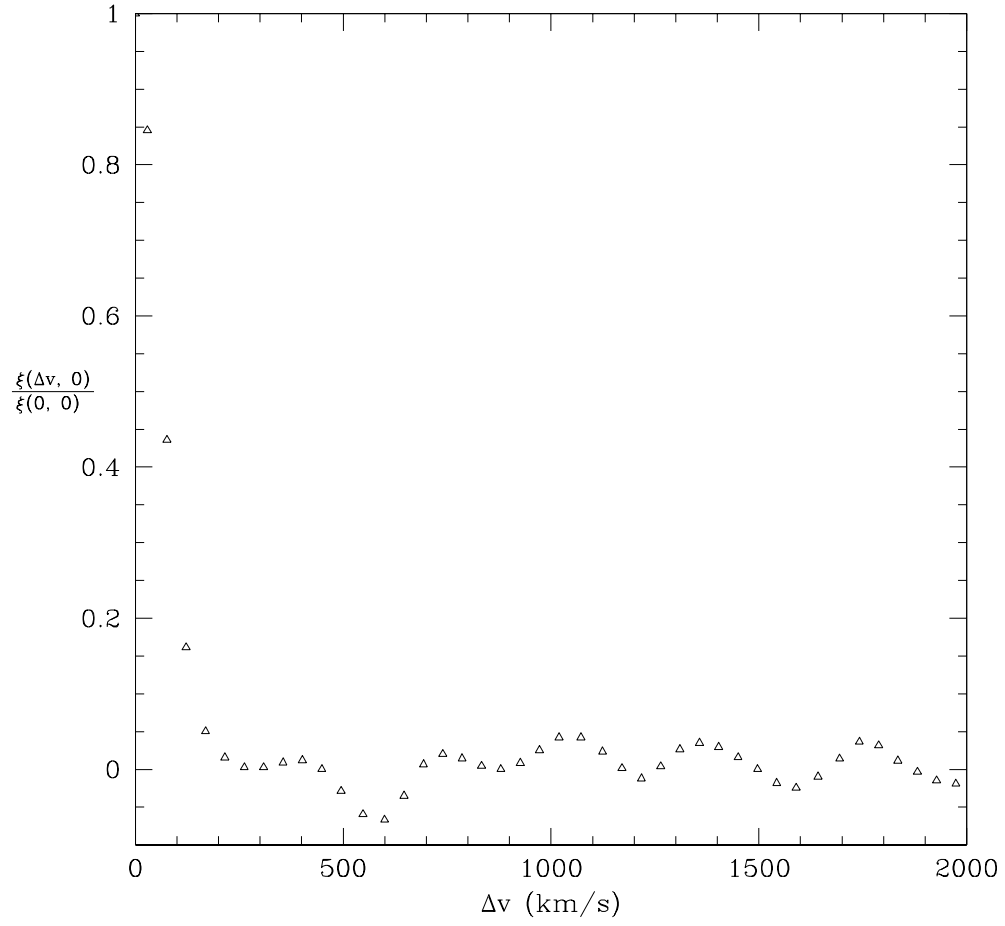


Fig. 5.— The correlation function along the line of sight for a pair of randomly generated spectra ($\Delta z = 0.5$, $\langle z \rangle = 2.25$ for each).

independent, so we use a Monte Carlo technique. We introduce noise to the calculated correlation function of a model by adding the noise values of the correlation measured from spectra of randomly generated lines (i.e., we sum the curves in Fig. 3 and 5). We then fit the five parameters of the model, minimizing the χ^2 of the correlation function in linear bins of $\sim 45 \text{ km s}^{-1}$, using the error bars found from the dispersion in the correlation obtained from the spectra of random lines. We repeat this procedure independently 25 times and fit each of the 25 simulated correlation functions separately. This should give the range of the fitted values we would expect to obtain from data with some fixed true parameter values. We do not use the correlation function at separations less than 300 km s^{-1} , approximately the scale of non-linearities. Changing this restriction to 200 km s^{-1} results in a small improvement (particularly, tighter correlation between f and β), but does not substantially change our conclusions. Figure 6 shows the results for the $f(z) = 1.61$, $\beta = 0.6$ model, fit to the triplet of quasars described above.

To reduce the scatter, it is necessary to add more quasars. Figure 7 shows the improvement that can be expected by combining multiple pairs of quasars at different angular separations (but still at the same redshift). Six pairs with separations $\Delta\theta = 45''$, $75''$, $105''$, $135''$, $165''$ and $195''$, with useful redshift range $z = 2.0 - 2.5$, are combined. In Figure 8, we use the same 6 angular separations but reduce the noise in the cross-correlation by a factor of two, and reduce the noise in the LOS correlation by a factor of six. This should approximately represent 24 pairs of quasars, with an additional 384 single quasars included to improve the measurement of the line of sight correlation. An independent determination of β can also improve the measurement of f . In Figure 9 we plot the distribution of measured f for $\beta = 0.2$, $\beta = 0.6$, and $\beta = 1.0$. For these fits, the value of β is fixed at the correct value. The sets of quasars used are the 6 pairs of Figure 7. Finally, with fixed β , we found that f can be measured to $\sim \pm 10\%$ (1σ) using the reduced noise (24 quasar pairs) of Figure 8.

4. Discussion

We have presented a method for analyzing the Ly α forest spectra along parallel lines of sight in order to extract the geometric parameter $f(z)$ and the quantity determining the strength of peculiar velocity distortions $\beta(z) \simeq \Omega^{0.6}/b$. We have worked here in the context of the linear regime, where the correlation function is small and the peculiar velocities generally cause large-scale structures (with positive or negative density fluctuations) to be flattened along the line of sight. Using the Gaussianization technique of Croft et al. (1998), one can measure the full redshift space correlation function and obtain β and $f(z)$. Using a model in which we distribute a realistic set of discrete lines randomly in space we have estimated the statistical errors expected for a measurement of the correlation function. We estimate that dozens of pairs of quasars are needed to reliably distinguish competing cosmological models.

The parameter f should probably be easier to measure going to smaller separations, in the non-linear regime. The amplitude of the correlation is then much larger, so many fewer pairs of

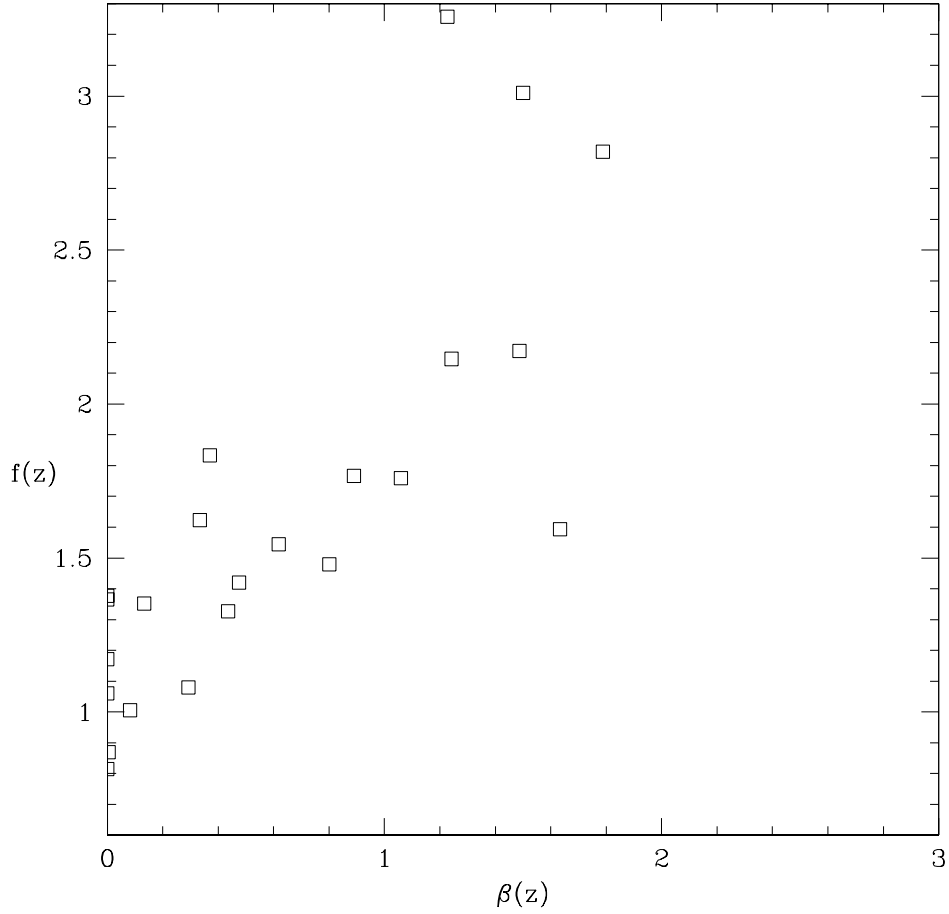


Fig. 6.— Best fit values for $\beta(z)$ and $f(z)$ for 25 sets of random spectra. The sets of quasar spectra fit were random realizations of a triplet with angular separations $127''$, $147''$, and $177''$, with a useful redshift range $z = 2.0 - 2.5$. The true values were $\beta(z) = 0.6$ and $f(z) = 1.61$. $f(z) = 1.61$ corresponds to $\Omega_0 = 1.0$ and $\Omega_\Lambda = 0.0$ at redshift $\langle z \rangle = 2.25$. Two points with high β do not appear on the plot. The constraint $\beta \geq 0$ was applied to the fits.

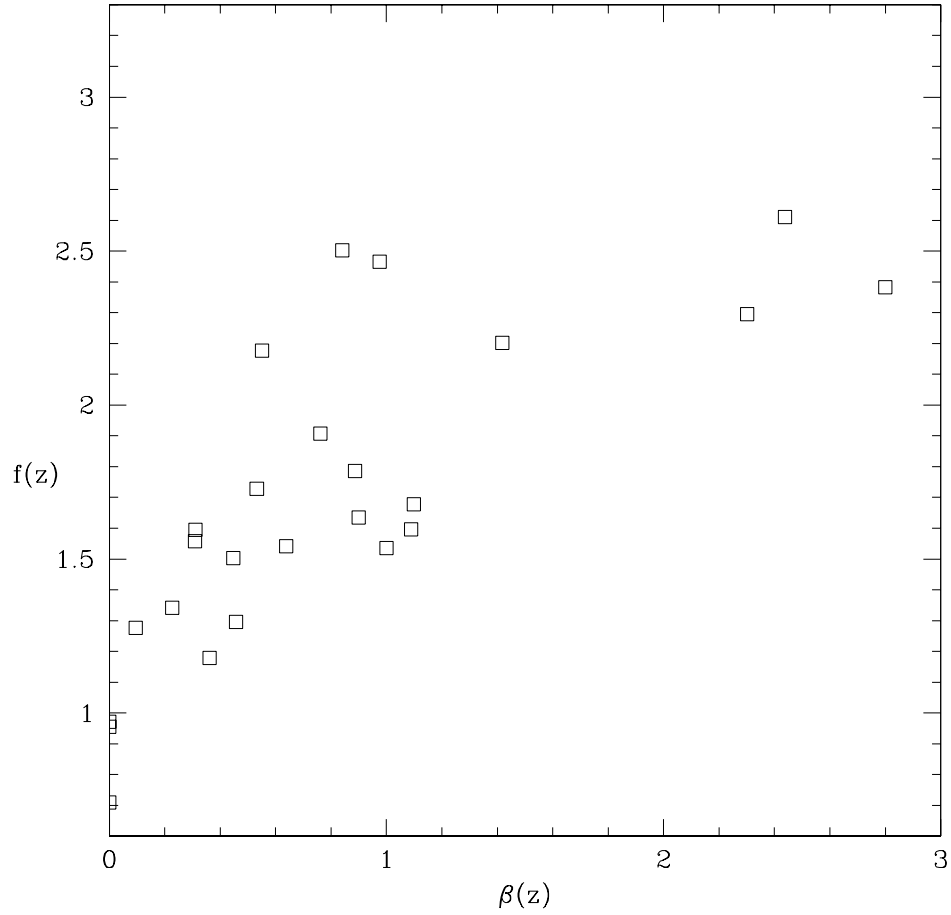


Fig. 7.— Best fit values for 25 realizations of a combination of 6 pairs of quasars separated by $\Delta\theta = 45''$, $75''$, $105''$, $135''$, $165''$, and $195''$. The true parameter values were $\beta(z) = 0.6$ and $f(z) = 1.6$ ($\Omega_0 = 1.0$, $\langle z \rangle = 2.25$). The constraint $\beta \geq 0$ was applied to the fits.

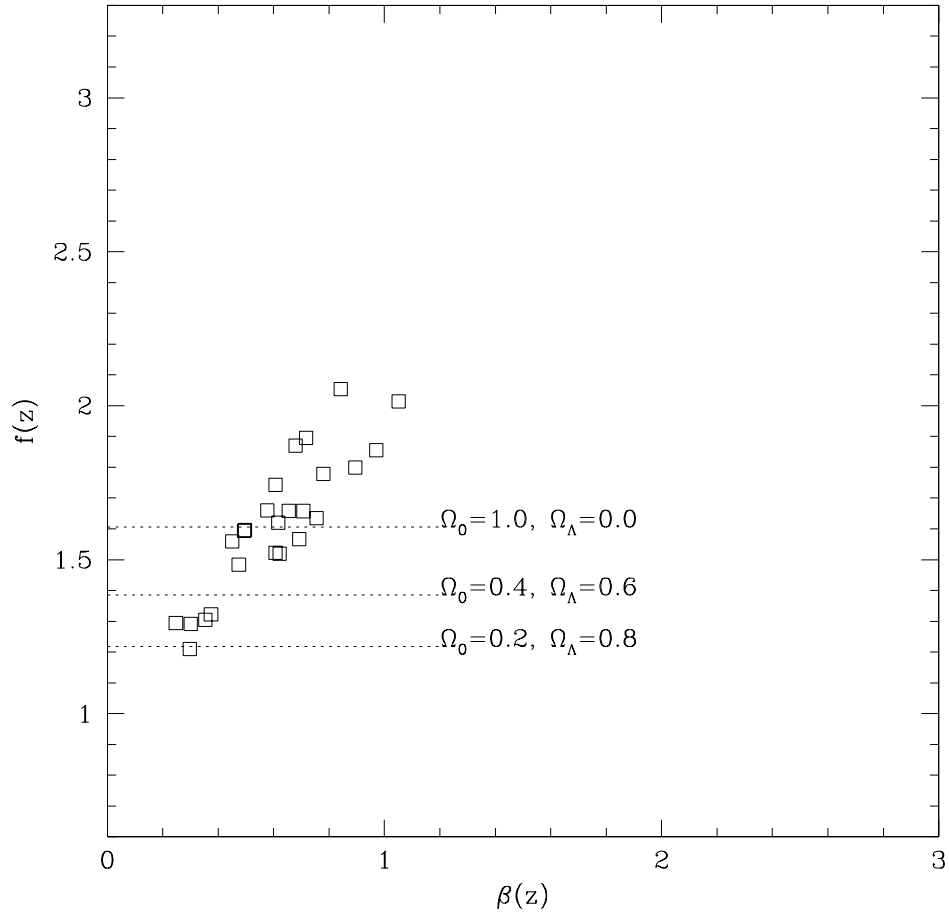


Fig. 8.— This figure shows the same 25 fits as Fig. 7, except the added noise in the cross-correlation has been reduced by a factor of 2, and the added noise in the line of sight correlation has been reduced by a factor of 6.

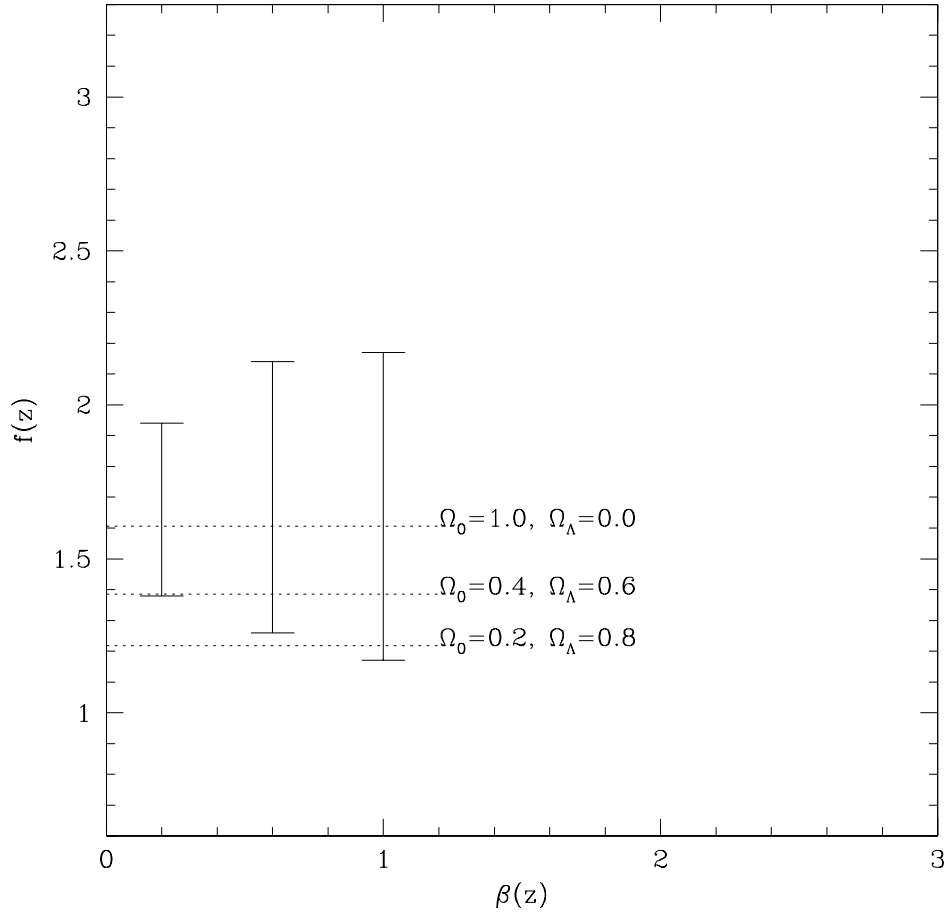


Fig. 9.— Fits assuming β is known (β is held fixed at the correct value). The error bars represent approximately 92% confidence. The 25 sets of quasars fit each contained 6 pairs as in Fig. 7. The true value of f is $f = 1.6$. The error bars exclude one point at each extreme. We show $\beta = 0.2$, $\beta = 0.6$, and $\beta = 1.0$.

quasars should be needed to measure the anisotropy of the correlation function to a fixed relative accuracy, required to constrain f to interesting levels. For small separations, the effect of peculiar velocities should be opposite to that in the linear regime: the correlation function should be elongated along the line of sight. This is caused by the well-known “fingers of God” effect in galaxy redshift surveys (where high density clusters appear as highly elongated filaments pointing toward us). In the Ly α forest, the “fingers of God” effect is simply the contribution of the internal velocity dispersion (either hydrodynamic or thermal) of the absorbers to their width.

The disadvantage of working in the non-linear regime is that the anisotropy of the correlation function can only be predicted with numerical simulations; in addition, the 2-point joint probability function is no longer given by equation (9), because the density field is no longer Gaussian. Therefore, we can only measure f if we can be certain that numerical simulations are accurate enough. But a more important reason to measure the 2-point function in the non-linear regime is probably that it will provide a very powerful test of the results of numerical simulations, and the large-scale structure theories in which they are based. If the Ly α forest arises from individual, high-density clouds, the fingers of God should be much more elongated and common than in the modern theories of gravitational instability from primordial fluctuations. Essentially, the full redshift space 2-point function gives a more quantitative version of the measurement of transverse sizes of the absorbers from coincidences of lines (Crotts & Fang 1998 and references therein).

On the large scales, an alternative to finding a large number of pairs of bright quasars to measure the anisotropy of the linear correlation function to high accuracy could be to work with spectra of much fainter, but much more numerous sources. So far, observational studies of the Ly α forest have used bright quasars as sources because of the desired high resolution and signal-to-noise that is necessary to measure the properties of individual absorption lines. But the correlation function could in principle be obtained from spectra of much poorer quality, as long as a very large number of spectra are taken. Recently, large numbers of galaxies are being identified at high redshift with the method of the Lyman limit break technique (Steidel et al. 1996). Spectra are now being taken routinely of galaxies in the redshift range 2.5 to 4, which have a number density of \sim one galaxy per square arc minute (Steidel et al. 1998). If the stellar continuum of the galaxies can be modeled, the Ly α forest spectra in these galaxies could provide a better way to measure the Ly α forest correlation on large scales (in this case, Gaussianization could not be used because the transmitted flux is measured only with very poor resolution, so numerical simulations would be necessary to predict the correlation function of the smoothed transmitted flux). These observations could also be used to study the cross-correlation of the Ly α forest with the Lyman limit break galaxies.

Future work is needed along two paths: analysis of numerical simulations and observational data. CWKH showed that the Gaussianization method works fairly well when applied to numerical simulations. Direct application of the full method to recover the redshift space correlation function to numerical simulations should indicate the effect of non-linearities and give a more accurate estimate of the accuracy that can be achieved in the observational determinations. The effect of

the finite size of the numerical simulations should now also be more easily understood, since the analytic method used in this paper predicts how the correlation should behave on the large scales.

REFERENCES

- Alcock, C., & Paczyński, B. 1979, *Nature*, 281, 358
- Ballinger, W. E., Peacock, J. A., & Heavens, A. F. 1997, *MNRAS*, 282, 877
- Bardeen, J. M., Bond, J. R., Kaiser, N., & Szalay, A. S. 1986, *ApJ*, 304, 15
- Croft, R. A. C. 1998, private communication
- Croft, R. A. C., Weinberg, D. H., Katz, N., & Hernquist, L. 1997, *ApJ*, 488, 532
- Croft, R. A. C., Weinberg, D. H., Katz, N., & Hernquist, L. 1998, *ApJ*, 495, 44 (**CWKH**)
- Crotts, A. P. S., & Fang, Y. 1998, *ApJ*, in press (astro-ph/9702185)
- Fisher, K. B. 1995, *ApJ*, 448, 494
- Hamilton, A. J. S. 1992, *ApJ*, 385, L5
- Hui, L. 1998, preprint (astro-ph/9807068)
- Hui, L., & Gnedin, N. 1997, *MNRAS*, 292, 27
- Kaiser, N. 1987, *MNRAS*, 227, 1
- Kaiser, N. & Peacock, J. A. 1991, *ApJ*, 379, 482
- Kim, T., Hu, E. M., Cowie, L. L., & Songaila, A. 1997, *AJ*, 114, 1
- Lilje, P. B., & Efstathiou, G. 1989, *MNRAS*, 236, 851
- Ma, C. 1996, *ApJ*, 471, 13
- Matsubara, T. & Suto, Y. 1996, *ApJ*, 470, L1
- Peebles, P. J. E. 1993, *Principles of Physical Cosmology* (Princeton University Press)
- Riess, A. G., et al. 1998, *AJ*, in press (astro-ph/9805201)
- Steidel, C. C., Adelberger, K. L., Dickinson, M., Giavalisco, M., Pettini, M., & Kellogg, M. 1998, 492, 428
- Steidel, C. C., Giavalisco, M., Pettini, M., Dickinson, M., & Adelberger, K. L. 1996, *ApJ*, 462, L17
- Weinberg, D. H. 1992, *MNRAS*, 254, 315